Automatic identification of streamlined subglacial bedforms using machine learning: an open-source Python approach

Ellianna Abrahams *[1] , Marion McKenzie *[2] , Fernando Pérez[1], Ryan Venturelli[2]

[1]Department of Statistics, University of California, Berkeley, California, United States

[2]Department of Geology and Geological Engineering, Colorado School of Mines, Colorado, United States

*These individuals contributed equally to this work and should be considered co-first authors. Please contact Marion McKenzie (marion.mckenzie@mines.edu | @mmglacialgeo on Twitter) or Ellianna Abrahams (ellianna@berkeley.edu | @SeeTheStarsRise on Twitter) with regard to this preprint.

Note This paper has not been peer reviewed and is being submitted as a preprint to EarthArXiv. The below manuscript has been submitted to *Boreas* for consideration within their special edition “Subglacial environments: Process, deposits, and landforms”.

Received: Added at production | Revised: Added at production | Accepted: Added at production

DOI: xxx/xxxx

ARTICLE TYPE

Automatic identification of streamlined subglacial bedforms using machine learning: an open-source Python approach

Ellianna Abrahams[*1] | **Marion McKenzie**[*2] | **Fernando Pérez**[1] | **Ryan Venturelli**[2]

[1]Department of Statistics, University of California, Berkeley, California, United States

[2]Department of Geology and Geological Engineering, Colorado School of Mines, Colorado, United States

[*] These individuals contributed equally to this work and should be considered co-first authors.

Correspondence

Corresponding authors Marion McKenzie
Email: marion.mckenzie@mines.edu and
Ellianna Abrahams
Email: ellianna@berkeley.edu

Abstract

Subglacial processes exert a major control on ice streaming. Constraining subglacial conditions thus allows for more accurate predictions of ice mass loss. Due to the difficulty in observing large-scale conditions of the modern subglacial environment, we turn to geologic records of ice streaming in deglaciated environments. Morphometric values of streamlined subglacial bedforms provide valuable information about the relative speed, direction, and maturity of past ice streams and the relationship between ice streaming and subglacial erosion and deposition. However, manually identifying streamlined subglacial bedforms across deglaciated landscapes, sometimes in clusters of several thousand, is an arduous task with difficult-to-control sources of variability and human-biased errors. This paper presents a new tool that utilizes a machine learning approach to automatically identify glacially derived streamlined features. Slope variations across a landscape, identified by Topographic Position Index, undergo analysis from a series of supervised machine learning models trained from over 600,000 data points identified across the deglaciated Northern Hemisphere (McKenzie et al. 2022). A filtered dataset produced through the combination of scientifically driven preprocessing and statistical downsampling improved the robusticity of our approach. After cross-validation, we found that Random Forest detected the most true positives, up to 94.5% on a withheld test set, while an ensemble average of models provided the highest stability when applied within the range of applicable datasets. We build these models into an open-source Python package, `bedmap`, and apply it to new data in the Green Bay Lobe region, finding the general ice flow direction and average streamlined subglacial bedform elongation with minimal effort. This type of open, reproducible machine learning analysis is at the leading edge of glacial geomorphology and will continue to improve with integration of newly acquired and previously collected data.

KEYWORDS

streamlined subglacial bedform, subglacial environment, machine learning, open science, glaciology

1 | INTRODUCTION

Redistribution and preservation of sediment in the subglacial environment provides a glimpse into controls on ice streaming and stability (e.g., Spagnolo et al. 2014 2017, Prothro et al. 2018, Simkins et al. 2018, Greenwood et al. 2021, McKenzie et al. 2022). Both erosional and depositional streamlined subglacial bedforms, elongate in the direction of ice flow, elucidate overlying ice controls of sediment distribution, ice speed (Stokes and Clark 2002, Stokes et al. 2013 2016), basal shear and slip speed (Zoet et al. 2021), and direction (Boulton 1976, Ottesen and Dowdeswell 2006, Roberts and Long 2005, Stokes and Clark 2002, Graham et al. 2009). Existing questions remain regarding the dominant glaciological and environmental controls on streamlined subglacial bedform evolution and presence (Zoet et al. 2021). In part, streamlined subglacial bedforms occur across a wide range of topographic and lithologic conditions (e.g., Greenwood and Clark 2010, Greenwood et al. 2021, McKenzie et al. 2022) and therefore have the ability to provide further insight to regional subglacial controls on ice streaming behavior. Due to the difficulty in observing streamlined subglacial bedforms in contemporary systems (e.g., Holschuh et al. 2020) and the similarities between streamlined features in deglaciated and contemporary areas of ice streaming (King et al. 2009), streamlined subglacial bedform across deglaciated landscapes have been used to make inferences about ice-bed interactions in modern glacial landscapes (e.g., Eyles et al. 2018, Greenwood et al. 2021, McKenzie et al. 2022). However, streamlined

subglacial bedforms often develop in clusters of up to several thousand features within a localized regions (e.g., Clark et al. 2018, Ely et al. 2016, Hughes et al. 2010), making mapping large areas an arduous and time-consuming task.

Previous work on mapping streamlined subglacial bedforms across deglaciated landscapes has been conducted manually (e.g., Principato et al. 2016, Norris et al. 2017), using Fourier spectra data (Spagnolo et al. 2017, e.g.,), through object-oriented automatic identification e.g., (Saha et al. 2011, e.g.,), contour-tree mapping (Wang et al. 2017), and by identifying slope variations in the landscape at various scales (e.g., McKenzie et al. 2022, Sookhan et al. 2021, Eyles et al. 2022). Each of these mapping techniques has associated error, where the most inconsistent error arguably stems from manual identification. Subjectivity in streamlined subglacial bedform identification can contribute to uncertainty that varies according the individual identifying the bedforms. Whereas automated or semi-automated techniques of streamlined subglacial bedform mapping also have error associated with feature identification and filtering, reproducible methods contribute to consistent error. Despite large advances in mapping deglaciated landscapes and using these data to interpret paleo-ice flow behavior, the use of machine-learning (ML) and artificial intelligence (AI) in landscape mapping to identify streamlined subglacial bedforms has been limited. Sookhan et al. (2021) developed an unsupervised K-means clustering approach to automatically identify streamlined subglacial bedforms, however the tools used to produce these results are not yet publicly available. The methods developed by Sookhan et al. (2021) seem highly effective in mapping large areas of ice streaming features in deglaciated landscapes and our work seeks to create a reproducible and accessible option to develop comparable results. Beyond this use-case of K-means clustering, ML and AI approaches in the field of glacial geomorphology may be currently limited due to a lack of a common data repository for previously collected data and no set data standards for the reporting of these data including data format, metadata details, and sharing practices. It is important to note, however, that although this lack of data standards and metadata makes re-use of previously collected data more difficult, a wide variety of practices are common due to a range in the interests for mapping deglaciated landscapes (Chandler et al. 2018). Typically, the purpose of data collection drives the decision-making processes behind metadata and data sharing. The history of streamlined subglacial bedform identification in the field of glacial geomorphology has resulted in an incredible number of glacial feature datasets that support the ability to interpret entire ice sheet histories from bedform assemblages, build understanding of processes that control bedform formation and evolution, contribute to identifying glaciation style, identify areas of interest for field campaigns, and provide constraints to ice sheet modeling (Chandler et al. 2018).

In this study, we present an open-source Python (Pérez et al. 2011) tool for the automatic identification of subglacial streamlined bedforms using a supervised machine learning (ML) approach trained on a dataset of 11,628 identified bedforms from McKenzie et al. (2022). In classification tasks, supervised learning approaches explore the optimal, or "best fit," solution to predicting the class of a set of observations constrained by the inherent hypothesis of the ML algorithm at play, which shapes the model's decision boundaries and final predictions. However, the individual hypotheses of single models may exhibit shortcomings in their specific fits, potentially resulting in overfitting and limited generalizability beyond the training dataset. Ensemble learning overcomes these limitations by consolidating the predictions of multiple models, thereby mitigating the weaknesses inherent in individual model fits. In particular, Random Forest (Breiman 2001), is a powerful ensemble algorithm that is well-suited for enhancing generalizability, and XGBoost (Chen and Guestrin 2016) is another ensemble algorithm that is known for improving prediction accuracy on lesser understood data at scale. While this study is a new application of these learning methods in the field of glacial geomorphology, Random Forest and XGBoost algorithms have been recently employed for other automated mapping applications in geology (e.g., Zhao and Chen 2023, Li et al. 2022, Ali et al. 2024) where they have both demonstrated high predictive performance.

Within this work, we share the end-to-end details of how we built our ML approach, deliberate designing it for generalized application. This approach ensures future applicability to unmapped regions of interest, even when they are beyond the initial training set. Section 2.1 details how we collected the training dataset used to train our ML models. In Section 2.2.1 we outline how we prepare the data for training using both statistical and scientifically driven methods for filtering spurious observations and downsampling confounding positive relief features. We find that combining scientifically informed filtering with a statistical downsampling approach improves automation more effectively than using each method independently. Sections 2.2.2 and 2.2.3 describe our ML model selection process, in which we find that our automated framework can recover the detection of up to $\sim 94\%$ of all glacial bedforms from Topographic Position Index (TPI) data products, or the slope variation detection developed for glacial landscapes by McKenzie et al. (2022). In 2.3 we develop our framework into an open source Python tool, compatible with ArcGIS TPI outputs, which we make publicly available and use to automate detection of glacially derived bedforms in a new location, a subset of the Green Bay Lobe area of ice streaming in Section 2.3.3. This approach is limited by the topographic and lithologic bed conditions of the streamlined subglacial bedforms included in the training dataset, and we therefore outline recommendations for its use in new regions of interest within Section 3.1. We show how this tool provides a further statistical confirmation for hypotheses on the relationship between ice streaming behavior and topology in Section 3.3, and how it can be employed to aid in speedily deriving ice flow speed and direction more efficiently from satellite DEMs in Section 3.4. Finally, in Section 3.5, we highlight upcoming directions for further tool development and call for data availability and open-access development of tools in glacial geomorphology applications to ensure continued progress in the age of open science.

This work has been designed to be reproducible and transferable to use-cases across other deglaciated landscapes that host bedforms as evidence of past ice streaming behavior. With this established workflow,

it is possible that our tool may provide a blueprint for applying similar methods to other geomorphic settings with repeating positive relief imprints on Earth's surface, such as sand dunes or mima mounds. We anticipate that these tools will have implications for the accuracy and efficiency of mapping streamlined subglacial bedforms across widely affected landscapes including many parts of Canada, Scandinavia, Chilean Patagonia, and potentially from the seafloor near margins of modern Antarctic and Greenland outlet glaciers. We share the scripts for our Python tool publicly on GitHub, release the data generated in validation on Zenodo, and store a stable version of the model code in the CryoCloud (Snow et al. 2023).

2 | METHODS AND RESULTS

We combine the methods and results sections in this work due to the inherently connected nature in our decision making process throughout the ML tool development. At each point, in order to determine robust and well-generalized next steps for our development pipeline, we utilize the results from previous steps. This workflow is highlighted in Figure 1.

2.1 | Data Collection

In 2022, McKenzie and others (McKenzie et al. 2022) identified 11,628 streamlined subglacial bedforms across nine sites in the deglaciated northern hemisphere (Figure 2). The geologic conditions of the nine sites were generally classified by bed conditions: soft, sedimentary or hard, crystalline/volcanic bedrock. The topographic conditions of each site were determined to be either "constrained" or "unconstrained" based on a 10 to 100 kilometer-wide analysis of surrounding landscape features (McKenzie et al. 2022). The sites are named and thus classified as A) the Puget Lowland of Washington, USA with mixed bed conditions and topographic constraints, B) Northwestern Pennsylvania, USA, C) Chautauqua, New York USA, D) M'Clintock Channel, Canada, and E) Prince of Wales Island, Canada all with sedimentary bed conditions and no topographic constraints, F) Nunavut, Canada with crystalline bed conditions and no topographic constraints, G) Bárðardalur, Iceland with volcanic bed conditions and topographic constraints, H) Northern Norway with crystalline bed conditions and topographic constraints, and I) Northern Sweden with crystalline bed conditions and no topographic constraints (Table 1). The primary bed conditions of the Puget Lowland are sedimentary deposits with some hard bedrock protrusions that affect ice flow behavior (McKenzie et al. 2023). For the purpose of our binary analysis in this work, the Puget Lowland site was reclassified as a sedimentary bed rather than a "mixed bed" due the primary presence of sedimentary deposits within the valley. The streamlined subglacial bedforms across these sites were developed during the Last Glacial Maximum (LGM) and are thought to have experienced minimal erosional reworking since their formation.

The dataset of streamlined subglacial bedforms from (McKenzie et al. 2022) was developed using digital elevation models ranging in resolution from 2 m vertical and 1.83 m x 1.83 m horizontal resolution to 10 m vertical and 30 m x 30 m horizontal resolution. The TPI tool employed by McKenzie et al. (2022) identified varying neighborhood-sized slope variations across a given elevation profile. These variations are then standardized and filtered to produce polygons from the positive landscape features. Post-TPI analysis, the 17,258 positive relief polygons that fit the morphometric standards for streamlined subglacial bedforms were manually filtered down to the final 11,628 true streamlined subglacial bedforms. From the analysis of TPI performance, with the exception of glacial features with millimeter to centimeter surface relief, almost all scales of known streaming bedforms (Ely et al. 2016) are identifiable by TPI (McKenzie et al. 2022). Highly elongate bedforms with low relief are the most difficult for TPI to identify. These type of bedforms may be found in regions with high preservation of non-glacial or minimally glacial landforms. This was the case in the crystalline bedrock sites of Sweden and northern Norway as older formations in the bedrock dominate the landscape (e.g., Ebert et al. 2012, Hall et al. 2013) and the LGM glacial features have much lower relief by comparison. Due to these challenges, streamlined subglacial bedforms across sedimentary sites, which have higher slope variations, are more likely to be identified by the TPI tool.

Prior to filtering and manual analysis of the TPI-identified features, there were over 600,000 polygons identified across all nine sites from McKenzie et al. (2022). This large, raw dataset was utilized in this new work to train the ML tool to identify which of the TPI polygons were glacially-derived streamlined bedforms. The training dataset of just over 600,000 rows includes information on bedform area, elongation, bedform long axis orientation, bedform length, bedform width, topographic conditions, geologic conditions, and whether or not the polygon was ultimately identified as a bedform. The training dataset is publicly available for others to use through GitHub and Zenodo datasets.

2.2 | A Case of Class Underrepresentation

In exploring the training-dataset TPI outputs, we find that our class of interest, the 17,258 streamlined subglacial bedforms, is a small fraction of the overall detected positive relief features. This inherent imbalance in class representation within the available training set leads to challenges in the application of ML models, since ML reward functions can prioritize overall statistical accuracy which includes correctly finding that something *is not* a glacially derived bedform. In our case, where the class of interest is $< 2.9\%$ of the overall data, the assignation of "not a bedform" would be measured as accurate $> 97.1\%$ of the time if an ML model hypothesized that the dataset did not contain any bedforms at all. Therefore without proper tuning, an off-the-shelf ML workflow would easily learn that it is typically correct to find that an input landform is not a glacial bedform, hindering accurate predictions of the bedforms we set out to classify. Class imbalance is a well studied field within the domain of classification statistics (See Rezvani and Wang 2023, for

TABLE 1 Site descriptions for the nine locations with streamlined subglacial bedforms used in the training dataset of the Random Forest, XGBoost, and the ensemble average of both models. Table adapted from (McKenzie et al. 2022).

Site	Conditions	Number of bedforms (*n*removed; *n*added)	Average orientation (degrees)	Average width ± std. (m)	Average length ± std. (m)	Average elongation	Average bedform area (km^2)
Puget Lowland, Washington state	closed topography sedimentary bedrock	1,978 (512;401)	34.47	365 ± 180	2,013 ± 1,261	5.9	0.52
Northwestern Pennsylvania	open topography sedimentary bedrock	881 (774;60)	149.70	162 ± 69	666 ± 342	4.4	0.08
Chautauqua, New York	open topography sedimentary bedrock	702 (493;103)	142.61	164 ± 77	652 ± 337	4.1	0.10
M'Clintock Channel, Canada	open topography sedimentary bedrock	1,737 (333;615)	45.98	278 ± 153	1,259 ± 789	5.0	0.33
Prince of Wales Island, Canada	open topography sedimentary bedrock	1,588 (1,657;665)	56.75	224 ± 162	1,054 ± 882	4.9	0.26
Nunavut, Canada	open topography crystalline bedrock	738 (>800;155)	150.42	115 ± 88	617 ± 614	5.4	0.09
Bárdardalur, Iceland	closed topography volcanic bedrock	659 (745;326)	132.36	175 ± 125	1,006 ± 701	6.6	0.13
Northern Norway	closed topography volcanic bedrock	1,427 (526;783)	106.50	132 ± 68	842 ± 580	6.9	0.11
Northern Sweden	open topography crystalline bedrock	1,918 (2,241;858)	75.44	346 ± 187	1,324 ± 794	4.1	0.43

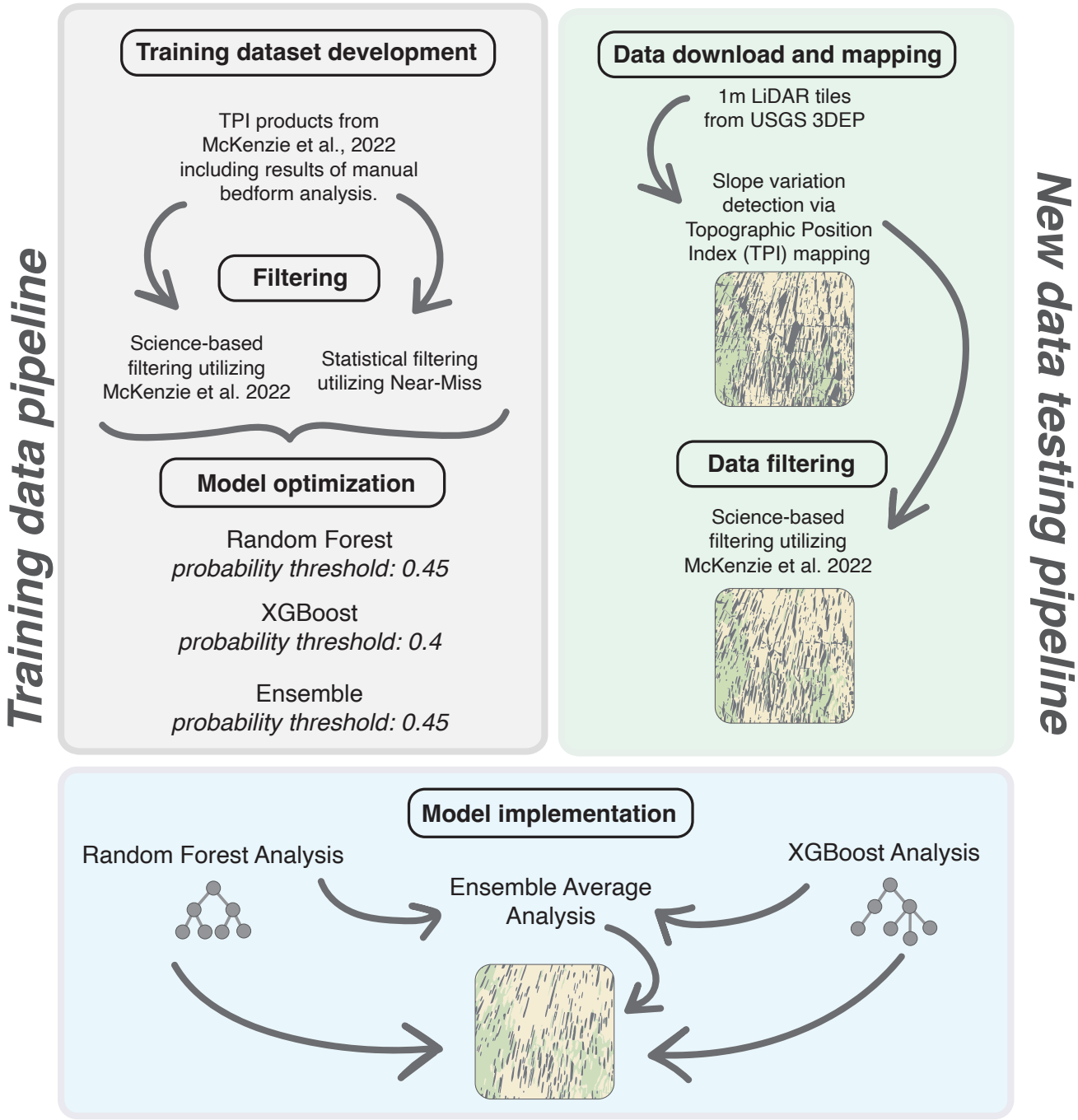

FIGURE 1 A visualization of our package framework. The training data pipeline on the left showcases our model development process, and the new data testing pipeline on the right illustrates the pathway for applying our framework to data in new regions.

a comprehensive review). Potential strategies include addressing underrepresentation at multiple stages of the ML pipeline, including the use of filtering, or undersampling, techniques as a data preprocessing stage before inputting data into a model (More and Rana 2017) and implementing algorithmic model approaches that iteratively minimize incorrect predictions, particularly on samples that the models find challenging to classify, like underrepresented classes. (Chen and Guestrin 2016).

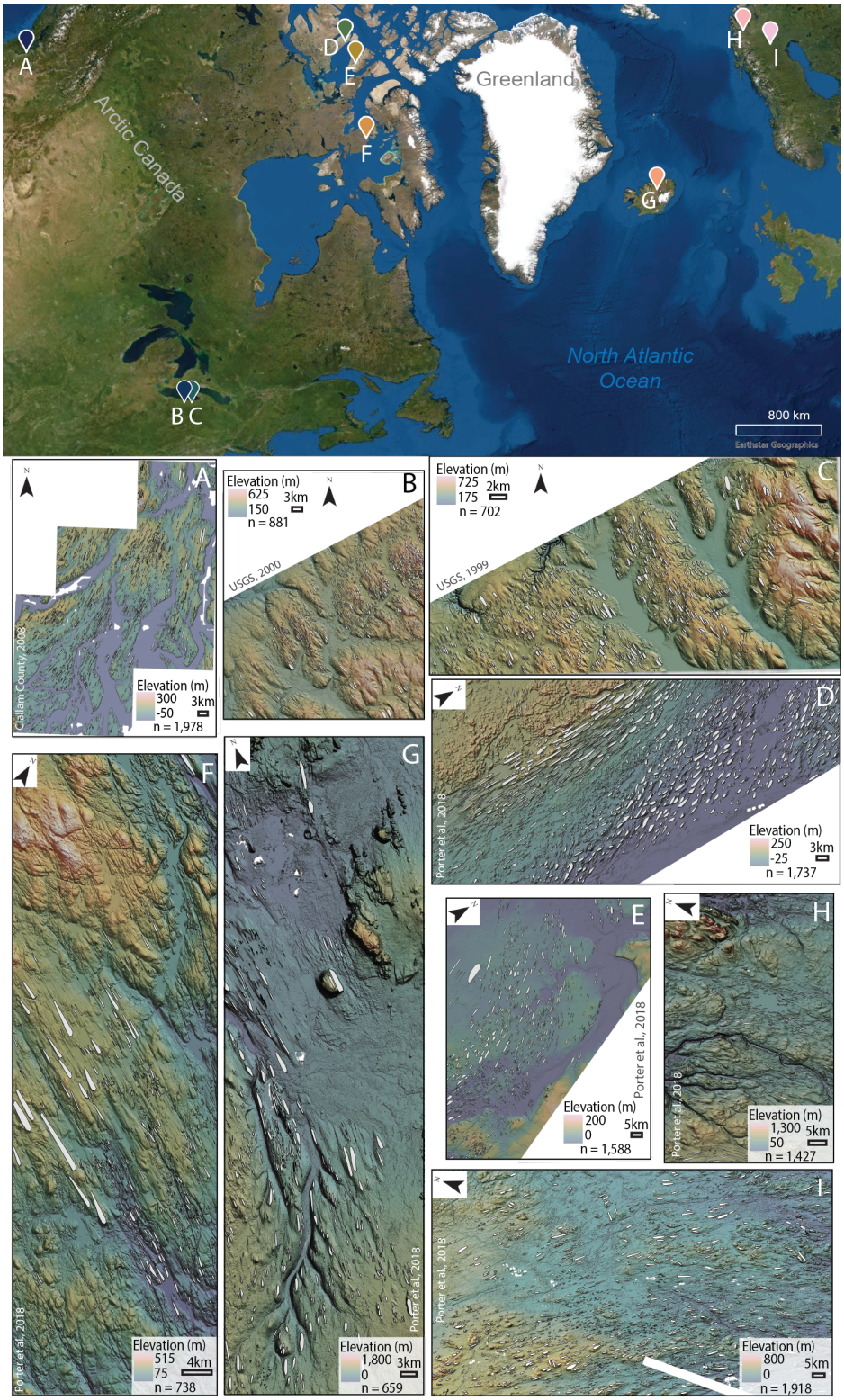

FIGURE 2 Sites included for streamlined subglacial bedform analysis including (A) Puget Lowland, Washington, United States; (B) Northwestern Pennsylvania, United States; (C) Chautauqua, New York, United States; (D) M'Clintock Channel, Canada; (E) Prince of Wales Island, Canada; (F) Nunavut, Canada; (G) Bárðardalur, Iceland; (H) Northern Norway; (I) Northern Sweden. Identified streamlined subglacial bedforms from both TPI and manual assessment are indicated by gray polygons. This figure has been adapted from the peer-reviewed work from McKenzie et al. (2022).

2.2.1 | Filtering the Non-Glacial Features to Balance Classes

We execute a scientifically driven filtering approach, as an algorithmic extension of manual data filtering in McKenzie et al. (2022), which we refer to as McKenzie et al. (2022) filtering. Individual filtering choices were made for each of the nine sites where bedforms were identified (Table 1). From the positive relief features identified across these landscapes by TPI, streamlined subglacial bedforms present as features elongate in the direction of ice flow, usually occurring in clusters with similar orientation. The smallest and largest seemingly glacially derived features were identified at each site, and filtering for feature length, width, area, and sometimes elongation ratio using ArcGIS Minimum Bounding Geometry, we narrowed the dataset to likely morphologies of glacially derived features. Orientation of ice streaming varies between site, but based on the primary cardinal direction of elongate feature clustering and likely direction of ice streaming, the TPI dataset was further narrowed to the features with a range of orientation that would indicate an origin from ice streaming. The filtering decisions that were made for each site have been incorporated in our Python workflow, and are made available on GitHub.

Testing for performance on a standard Random Forest model (Breiman 2001), we find that the McKenzie et al. (2022) filtering approach increases the representation of the glacial bedforms to 19.5% of the data, and improves the detection precision of bedforms by $> 29\%$. Even though this filtered dataset is still within the regime of class imbalance, previous studies have found that increasing the representation of fractional classes so that they make up a larger percentage of the overall set already improves model performance (Abrahams et al. 2024). To compare McKenzie et al. (2022) filtering to statistical approaches like random undersampling and Near Miss, we use the same representation ratio, so that in each method, we filter down the majority class so that it makes up a similar fraction the training data that McKenzie et al. (2022) filtering achieves. We find that all undersampling methods improve detection of glacial bedforms when compared to a Random Forest model trained on the unfiltered dataset. McKenzie et al. (2022) filtering outperforms the recall (i.e. finding correct bedform detections) of random undersampling, illustrating that the implicit inclusion of scientific knowledge that isn't caputured in our model specification is helpful in improving the detection of the patterns that describe glacial bedforms. Near Miss provides better stand-alone performance for the detection of glacial bedforms of the three individual filtering methods, but still fails to detect $\sim 1/4$ of glacial bedforms. Furthermore, one of the disadvantages of Near Miss is that it relies on prior knowledge of class assignment. While this makes Near Miss a useful approach to employ at training time, it cannot be used to preprocess a test set in a new region or on previously unclassified data, which is inherently missing knowledge of the class assignment.

To improve overall detection, so that our model is robust even when we cannot run Near Miss on new observations, we combine McKenzie et al. (2022) filtering with Near Miss to create our training set, downsampling the non-bedform features in the McKenzie et al. (2022) filtered dataset until the glacial bedforms are represented equally as often as other positive relief features. This combined approach, which incorporates both scientifically informed filtering (McKenzie et al. (2022) filtering) and increased statistical separation between both classes (Near Miss), easily outperforms all previous downsampling techniques, achieving near complete precision at high prediction probabilities. The combined approach finds 94.6% of the true glacial bedforms while correctly assigning a bedform 93.1% of the time.

Figure 3 visualizes the difference in detection performance between these four filtering approaches in a confusion matrix (Ting 2011). The diagonal of a confusion matrix indicates how often model predictions are correct (known as true positive detections and true negative detections), and the off-diagonal components indicate where the model is "confused," i.e. it misses detecting a bedform (lower left, known as a false negative detection) or incorrectly detects a bedform when a feature is some other landform (upper right, known as a false positive detection). We share the performance metrics for each of the filtering approaches in the upper portion of Table 2. These metrics measure how well our model fits predict the true assignation of glacial (or non-glacial) origin to landscape features. In other words, these metrics quantify if the model predicts correctly when a feature is glacial bedform and if it predicts correctly when a feature is not a glacial bedform. Due to the inherent class imbalance in the data, we place particular emphasis on improvements in the F1 score, which measures the strength of how often the model fit accurately predicts a glacial bedform compared to how often the model misses a glacial bedform or mistakes another landform feature for a bedform (see supplementary material A.1 for further explanation).

2.2.2 | Machine Learning Model Selection

Random Forest's strength lies in its ability to find generalizable patterns in complex data, which mitigates overfitting. This is useful when training on data that has been preprocessed in any way with Near Miss. XGBoost's strength lies in its ability to enhance predictive accuracy on lesser understood data, which, in contrast, mitigates underfitting. This is useful for capturing instances of a class that are missed in Random Forest classification. Given the strengths of both models, we test the application of both on our dataset and share the performance comparison between these approaches in the lower portion of Table 2.

We find that both the XGBoost and Random Forest approaches achieve similar statistical accuracy and, more importantly, the same F1 score, indicating that the balance between missed streamlined subglacial bedforms and other landforms mistakenly identified as streamlined subglacial bedforms is equal using either tool. However, Random Forest outperforms XGBoost in recall, which indicates the model's ability to avoid missing a streamlined subglacial bedform. In other words, fewer streamlined subglacial bedforms are absent from the Random Forest predictions. XGBoost outperforms Random Forest in precision, which indicates the model's ability to avoid mistaking other positive

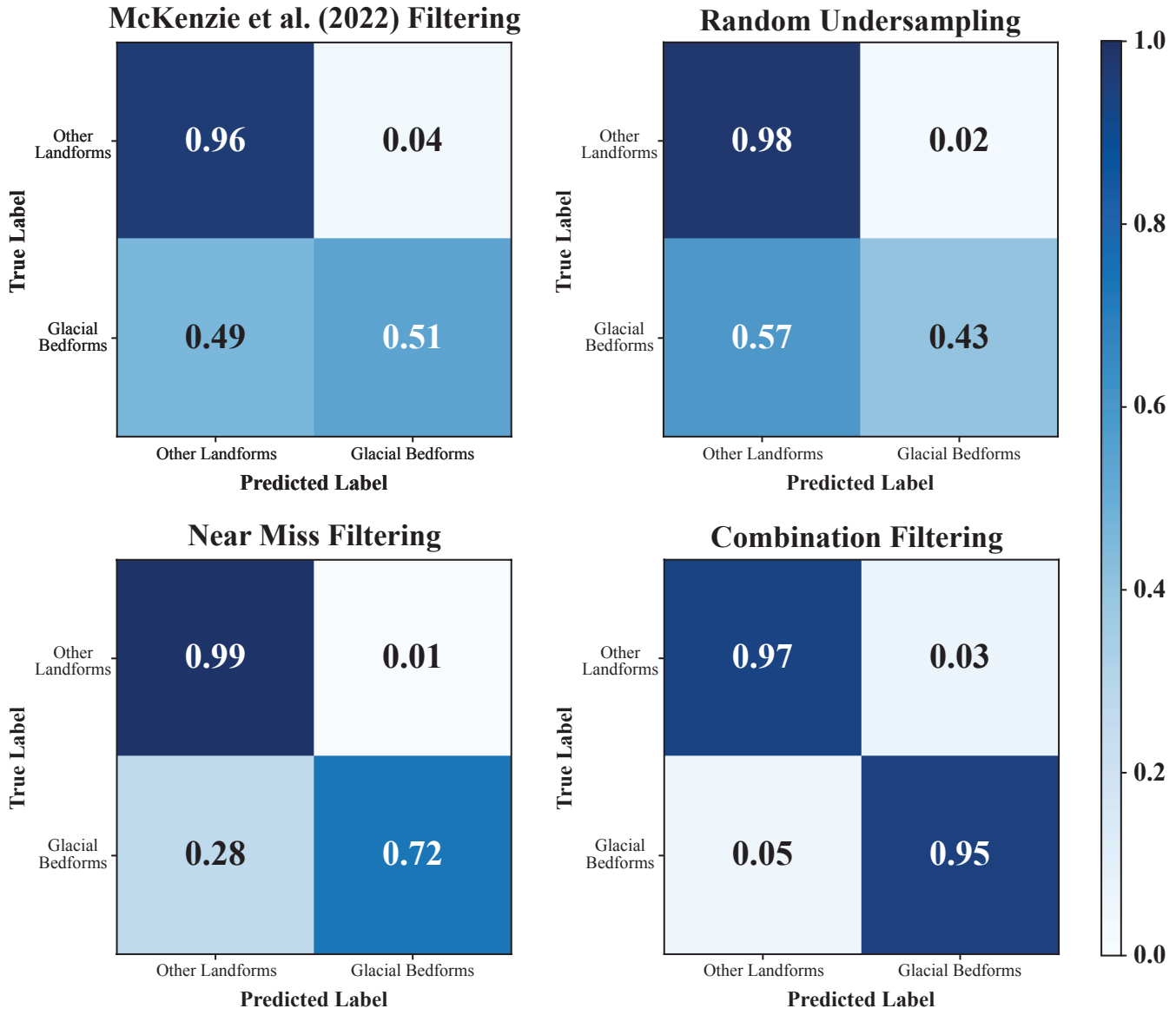

FIGURE 3 Confusion matrices for each of the candidate filtering methods (Section 2.2.1). A combined approach that incorporates both a scientifically driven filtering approach (McKenzie et al. 2022) with the class balancing approach of Near Miss (Mani and Zhang 2003) recovers 94% of true glacial bedforms, while only mistaking 3% of the bedform predictions.

relief features for bedforms. In other words, less of the XGBoost streamlined subglacial bedform predictions are incorrect. These results are not surprising as they play to the strengths of each of these model approaches. However, in our case, where this mapping tool is being built to automate the classification of not-yet-known streamlined subglacial bedforms in future studies, both false positives (mistaken bedforms) and false negatives (missing bedforms) are costly. For this reason, we test a third model approach that is well established in statistics, known as ensemble averaging (James et al. 2023). In this approach, we take the average of the probabilistic predictions from Random Forest and from XGBoost, essentially combining the best of both models, and we refer to this approach as Ensemble Average. In the final row of Table 2 we show that this approach improves upon the shared F1 score of the Random Forest and XGBoost models, indicating better balance between missed and mistaken bedforms.

While ArcGIS has native Random Forest and XGBoost implementations, we chose to implement these algorithms directly in Python (Pérez et al. 2011) on the CryoCloud (Snow et al. 2023) platform using the `scikit-learn` (Pedregosa et al. 2011) and `xgboost` (Chen and Guestrin 2016) libraries. We make this choice because the `scikit-learn` and `xgboost` libraries allowed for built-in optimization to find the best-fit hyparaparameters (the tuneable choices in a model specification like number of trees or the learning rate), which we detail below in Section 2.2.3.

TABLE 2 Glacial bedform prediction performance between different data filtering methods (upper table) and between different machine learning models on the highest performing filtering method (lower table). We find that a filtering approach that combines scientifically driven filtering (McKenzie et al. 2022) to remove site-specific spurious detections and statistical filtering to create more separation in the features that describe classes creates the most significant improvement averaged across performance metrics. When comparing candidate machine learning models on this filtering approach, we find that all display strong performance detecting more than 91% of glacial bedforms, and that an ensemble average between Random Forest and XGBoost predictions provides the best balance between false positive (mistaken glacial bedforms) and false negative (missed glacial bedforms) predictions as indicated by F1 score.

Performance Comparison Between Candidate Filtering Methods (Section 2.2.1)				
Method	Accuracy	Precision	Recall *(Correct Bedform Detections)*	F1 Score
Random Forest *McKenzie et al. (2022) Filtering*	87.0%	73.9%	51.0%	60.3%
Random Forest *Random Undersampling*	88.9%	79.0%	43.1%	55.8%
Random Forest *Near Miss Filtering*	95.2%	**97.5%**	72.1%	83.0%
Random Forest *Combined Filtering*	**95.7%**	96.8%	**94.6%**	**95.6%**
Performance Comparison Between Candidate Machine Learning Models (Section 2.2.2)				
Random Forest *Combined Filtering*	94.5%	94.2%	**94.5%**	94.3%
XGBoost *Combined Filtering*	94.5%	**94.7%**	94.0%	94.3%
Ensemble Average *Combined Filtering*	94.5%	94.3%	94.4%	**94.4%**

2.2.3 | Cross-validation of the Model Hyperparameters on McKenzie et al. (2022) Filtering

In statistical modeling, cross-validation is used to search across a grid of potential model hyperparameters (i.e. initial model choices like number of trees in a Random Forest or the learning rate in XGBoost; Geisser 2019). Such cross-validation moves the model closest to the optimal estimation of true positives. In a typical cross-validation approach, a k-fold is employed to withhold $1/k$ of the data for validation, while a series of models constructed from a grid of hyperparameters is trained on the remaining data. This process rotates through the grid k times until all of the data has been employed for training and testing in turns. The best-fit hyperparameters are selected as those that lead to the detection of the most true positives while optimizing on a chosen performance score averaged across the prediction outcomes from all k folds (James et al. 2023). The k-fold approach makes the assumption that the full dataset, regardless of a train-test split, describes any new dataset that we would choose to map with this model. In this study, we prepared training data using a combination of filtration methods: McKenzie et al. (2022) filtering which, being informed by the scientific metadata that describes a particular site, is conceptually replicable in any new site where TPI positive relief features are developed, and Near Miss, which instead is only replicable with advanced and manually derived knowledge of streamlined subglacial bedform true positives. We made the choice to balance the data at training time using a filtering approach that included Near Miss in order to guide the model towards the best fit, however we want to ensure that the final fit hyperparameters are optimized to achieve high performance on a realistic test set, one that is filtered using the methods from McKenzie et al. (2022) alone and is therefore replicable on new, previously unclassified data.

Using the dataset produced by both McKenzie et al. (2022) filtering and Near Miss filtering and the dataset developed solely by McKenzie et al. (2022) filtering, we tested each fit across a grid of candidate hyperparameters. In order to test across this grid, we employ `scikit-learn`'s customizable k-fold cross-validation approach to identify the optimal model fit. We define a 3-fold such that any set of observations that is available in both datasets is subdivided so it is not duplicated between training and testing time within any individual fold. The full explanation of this process is in Section A.2. We find that thresholding the Random Forest model to 45% probability, the XGBoost model to 40% probability, and the Ensemble Average to 45% probability all recover $\sim 75\%$ of the glacial bedforms but each approach has advantages and disadvantages in how many mistaken bedforms were detected and how many true bedforms were missed. In Figure 4a, we show the true positive rate vs. the false positive rate (TPR/FPR) across probability thresholds, also known as the ROC curve. The greater the area under the ROC curve (or area under curve, AUC), the more successful a model is at finding glacially derived bedforms without mistaking other landforms. Figure 4b, illustrates F1 score as a function of probability threshold. The maximum

of these curves indicate the best threshold to find the most bedforms while making the least overpredictions. The Ensemble Average, Random Forest, and XGBoost models from the cross-validation on withheld test data from McKenzie et al. (2022) are all shown in grey. We can see that in cross-validation, Random Forest shows the best performance both in TPR/FPR and in F1 score, but that Ensemble Average is nearly as stable and reaches similar performance. XGBoost underperforms in this case, but in Section 2.3.3, we highlight a case on a new region where XGBoost outperforms Random Forest.

To enable reproducibility of our results and future usage of our learned models to predict bedforms in other datasets, we share the best fit models for each of these approaches on CryoCloud (Snow et al. 2023) and on GitHub.

2.3 | An Open-source Python Framework to Complement an ArcGIS Workflow

Automated pipelines, such as the one presented in this study, mitigate human error by explicitly defining the constraints and parameters used to identify glacially derived bedforms. This automation reduces subjective errors associated with manual identification. Our objective was to develop tools that enable future research to use the same automated process, thus standardizing bedform classification in glacial geomorphology. This approach ensures complete reproducibility of our results in line with the Findability, Accessibility, Interoperability, and Reuse (FAIR) data standards (Wilkinson et al. 2016) and allows for in-distribution comparison with future bedform detections. We have integrated these automated pipelines into an accessible, open-source Python too, that is compatible with ArcGIS TPI outputs, as detailed in the following sections.

2.3.1 | An open access Python package for bedform prediction

We built a Python package, `bedmap`, that is compatible with Python $\geqslant 3.9$, is publicly available on the Python Package Index, and is versioned in Zenodo. This script takes in positive relief detections from TPI outputs that are saved as a Comma Separated Values (csv) from ArcGIS shapefiles. TPI output csv files require columns named `Topo`, describing site-defined topographic conditions as either "O" for open or "V" for closed, `Bed`, describing the site-defined bed characteristics as either "S" for sedimentary or "C" for crystalline/volcanic, `Area`, comprised of individual feature areas calculated in ArcGIS, `Elong`, comprised of individual feature elongation calculated from feature length and width values in ArcGIS, and original feature identification number (*ORIG$_F$ID*) column so individual features can be linked back to ArcGIS visualization after model analysis. The package can be used to implement the full testing branch of the workflow shown in Figure 1. The `McKenzieFiltering` function can be implemented to prefilter the full set of the TPI-generated training data as a preprocessing step following the protocol outlined in Section 2.2.1, and the `ClassifyBedforms` function allows users to choose between applying the Random Forest, XGBoost, or Ensemble Average model fits, described in Sections 2.2.2 and 2.2.3, to automatically detect bedforms in new areas of interest.

Within Python, users can choose a probability threshold based off their particular application, following the recommendations in Section 3.1. Users also have the option to output the probability that a detection is a bedform as predicted by their model of choice or as a final thresholded binary prediction. We include the source files for the `bedmap` package, documentation for implementing this tool on new data, and full descriptions of package usage on GitHub. Example implementation Jupyter notebooks (Granger and Pérez 2021) are also made available there and on CryoCloud (Snow et al. 2023).

2.3.2 | Utilizing ArcGIS for bedform prediction

McKenzie et al. (2022) published a TPI tool built with ArcPython and ArcGIS Model Builder. We expand this ArcGIS tool by integrating necessary `bedmap` model components into the output of the ArcGIS Model Builder pipeline. We chose not to implement the `bedmap` package within an ArcGIS framework directly due to internal dependencies on open source Python packages like `joblib` and `scikit-learn`, and the inability to import our `bedmap` module. While these can be installed to ArcGIS by updating the Python path at the base of a user directory, this path differs from computer to computer and modifying system-wide paths can have unintended consequences and complications. Updating the path properly requires advanced computing knowledge, and we wanted to make our tool as widely accessible as possible to users at all levels of computational ability. Therefore, after the automated TPI pipeline (McKenzie et al. 2022) is implemented on an input DEM, TPI output should be filtered using McKenzie et al. (2022) filtering concepts as outlined in Section 2.2.1. This filtered datset should be exported as a .csv file with the necessary columns for input in the Python module.

After bedform prediction is completed using our Python framework (see Section 2.3), the output .csv file with column of predicted bedforms may be re-uploaded into ArcGIS using the "Add Data" feature. Users can then "Join" the model output .csv file with the original TPI feature shapefile through the shared "*ORIG$_F$ID*" column. This join will allow for users to visualize the specific positive relief features that were predicted to be glacially derived bedforms using the Random Forest, XGBoost, or Ensemble Model tools.

2.3.3 | Model validation through a subset of Green Bay Lobe bedforms

While our statistical tests ensure the Random Forest and Ensemble Average tools are robust and able to identify streamlined subglacial

bedforms across previously studied deglaciated landscapes with variable bed and topographic conditions, we showcase the ability for our tool to identify streamlined subglacial bedforms in a new site that is not represented in the distribution of our training set. We identified a subset of streamlined subglacial bedforms from the Green Bay Lobe between 88.6023015°and 89.0969540°West and 43.5172629°and 43.2489431°North using our automated ArcGIS Model Builder for calculating TPI and using those outputs with our Python pipeline. Final visualization was developed by re-uploading the Python output predictions into ArcGIS and "Joining" the predicted bedform output to the original TPI feature shapefile through the "$ORIG_FID$" column 5.

The region of interest for tool validation is comprised of dolomite, limestone, and shale of Ordivician age with up to 30 meters of unconsolidated deposits from glaciation (Mudrey et al. 1982). The LGM flow regime of the Green Bay Lobe appears to be generally unimpeded by underlying topography in this region, therefore the Green Bay Lobe site was classified as a sedimentary bed system in a topographically unconstrained area. One meter DEMs of the area of interest were available from the USGS 3DEP Elevation program[†]. TPI analysis of the landscape produced 157,011 positive relief features across the landscape (Figure 5). Following McKenzie et al. (2022) filtering protocols, we downsampled the original dataset to only include features with an orientation between 2 and 180 degrees, indicating the primary direction of ice streaming. We filtered the raw dataset to include features with a length between 140 and 4000 meters, width between 20 and 500 meters, and areas between 8000 and 850,000 square meters. All of these classifications represent the most realistic morphometrics of glacially derived features in this region based on our initial visual assessment. After filtering, the dataset input for the model was then comprised of 3,186 positive relief features (Figure 5). Finally we applied the Ensemble Average, Random Forest, and XGBoost models to the remaining filtered features to automate the detection of streamlined subglacial bedforms. Figure 5 visualizes the application of each step of this workflow on the map of Green Bay Lobe.

In order to determine model accuracy in this new region, we manually analyzed the TPI dataset to determine which identified positive relief features were streamlined subglacial bedforms. The final dataset used for model assessment is comprised of 945 manually identified streamlined subglacial bedforms. We compared our manually determined dataset (with its own associated subjective errors) to the estimated outcomes predicted by our Random Forest, XGBoost, and Ensemble Average models. Random Forest identified 1,285 streamlined subglacial bedforms with 77% accuracy as compared to the manually identified features. XGBoost identified 1,251 streamlined subglacial bedforms with 79% accuracy. Ensemble Average identified 1,155 streamlined subglacial bedforms with 78% accuracy. Figure 4 shows the ROC curve and the F1 score as a function of probability for each of these models. We can see that XGBoost (shown in the blue dash-dotted line) provides the best performance, as illustrated by the highest AUC and F1 score, but in both metrics, Ensemble Average (purple solid line) provides a close second. This is in contrast to the model performance at cross-validation time, which was evaluated on a withheld test set of the regions identified in (McKenzie et al. 2022). In that case, Random Forest (grey dashed line) provided the best performance, and XGBoost provided the poorest performance (grey dash-dotted line). However, similar to the training dataset, Ensemble Average provided a stable and close second to the highest performing model. For this reason, we recommend Ensemble Average at a threshold of 45% probability as the model of choice for new regions.

[†] More information about this program can be found at the USGS website, linked here

3 | DISCUSSION

We discuss the interdisciplinary approach to landscape analysis presented in this work, and explore the intersection of the fields of glacial geomorphology and spatial statistics while defining best practices for the application of our approach to new regions. To showcase the workflow, we present the application of this tool to the Green Bay Lobe site. Results from this work provide implications for determining controls of subglacial conditions on ice streaming behavior. We end by commenting on the future development of these tools, which will only improve with the addition of new data, and the importance of open science in glacial geomorphology and spatial statistics integration.

3.1 | Usage Recommendations for the `bedmap` Package

Identifying streamlined subglacial bedforms accurately is essential for glacial geomorphic studies and the inferences scientists are able to make about subglacial controls on ice behavior from these features in the geologic record. To automate the detection of these bedforms from TPI-identified positive relief features, we investigated classified bedforms from nine sites with varying topographic and lithologic conditions, enhancing the applicability of the tool (McKenzie et al. 2022). We developed the Python package `bedmap`, which offers flexible and robust bedform detection approaches from positive relief features identified across the surface. Our developed framework includes data preparation guidelines, model selection advice, and probabilistic prediction thresholding to ensure reliable bedform identification across diverse landscapes. By following these usage recommendations, researchers can effectively use TPI and `bedmap` even in challenging terrains.

We outline some features of our Python framework, `bedmap`, and identify recommended usage pathways here.

1. **Preparing the Data** As `bedmap` was validated on data that used McKenzie et al. (2022) filtering, we recommend that any new data undergo similar conceptual filtering. If new sites overlap in region with those used in McKenzie et al. (2022), use the appropriate filtering schema for that particular region by running the `McKenzieFiltering` routine in `bedmap`. When employing `bedmap` on

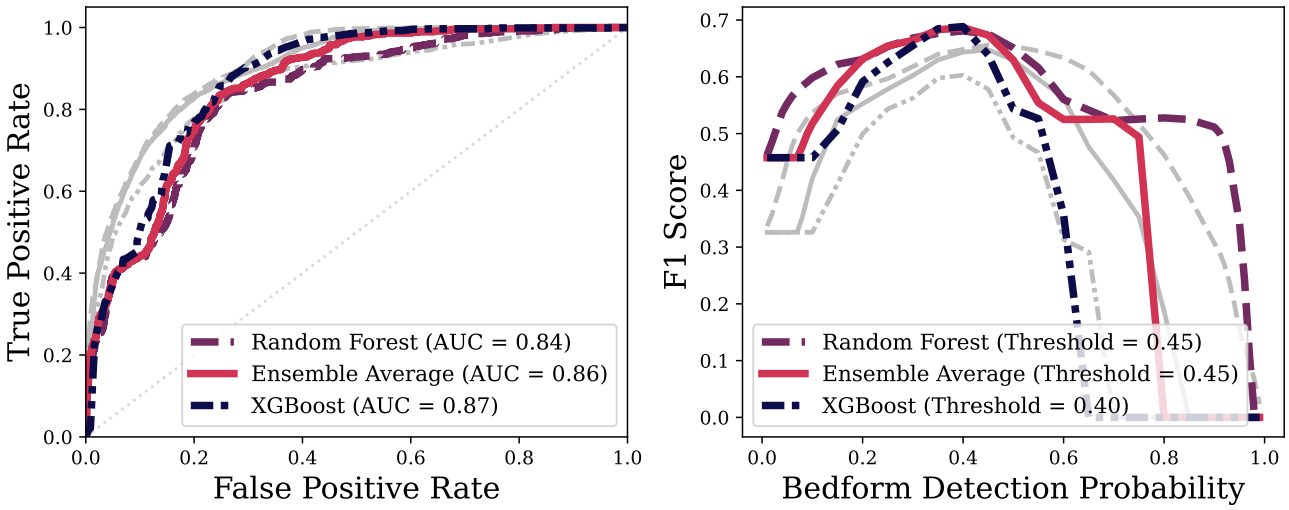

FIGURE 4 Identification rates and F1 scores versus probability scores for all three models, tested on a section of the Green Bay Lobe ice stream (shown in blue, purple, and magenta) and on the withheld cross-validation test set (shown in grey). In the ROC curve on the left, higher AUC indicates higher performance. XGBoost (blue dash-dotted line) provides the best performance on the new data in the Green Bay Lobe but the poorest performance on data from the withheld test set during cross-validation (grey dash-dotted line). In contrast, Random Forest (magenta dashed line) displays the poorest performance in the Green Bay Lobe, but the highest performance at cross-validation time (grey dashed line). However, in both cases, Ensemble Average provides a close second to the highest performing model making it an ideal model choice for new regions where glacially-derived bedform locations are unknown.

a new region, Section 2.2.1 outlines the choices made in McKenzie et al. (2022) filtering; we recommend employing a similar filtering scheme for new regions to keep data within the validated limits of the model. Data should be exported from ArcGIS as a .csv file and include necessary columns of information as outlined in 2.3.

2. **Model Selection** We offer three potential model choices in `bedmap`: Random Forest, XGBoost, and the ensemble average of the two. In new regions, where bedforms are not yet identified, we recommend employing Ensemble Average. Ensemble Average provides stable performance when it is unknown whether a region might lead to more false positives or negatives. While Figures 4 and 5, show cases of Random Forest and XGBoost providing the best performances respectively, in each case Ensemble Average was near to top performance, and the top performer was only identifiable because true bedforms were known.
3. **Thresholding Probabilistic Predictions** All `bedmap` predictions can be output either as a percentage probability of the positive relief feature being glacially derived, or if the user chooses, as a binary prediction. The binary predictions are determined by thresholding the probability at a chosen percentage. By cross-validating the data (Section 2.2.3) we find that the optimal prediction threshold for Random Forest is 0.45, for XGBoost is 0.4, and for Ensemble Average is 0.45. These optimized thresholds are the default usage case for each model in `bedmap`, but the prediction thresholds may be also be manually overwritten.
4. **Comparison Between Models** Each model approach included in `bedmap` has comparative strengths and weaknesses. Where possible, we recommend running inferences from all three model fits and comparing the results to reduce the need for manual post-processing. This allows users to benefit from the strengths within each model approach.

3.2 | Model limitations

Previous work has shown that the TPI tool used to compile our training set performs most poorly in regions with highly elongate bedforms with low surface relief (McKenzie et al. 2022). The narrow slope differentiations make the positive relief features more difficult for TPI to identify. Landscapes where evidence of ice streaming is minimally preserved or where there are prominent non-glacial landforms usually requires a higher amount of manual mapping due to a lack of TPI accuracy. Streamlined subglacial bedforms that were missed by TPI identification were more frequently located on crystalline bed surfaces in Norway, Sweden, and Iceland, possibly due to landscape legacy preservation with higher relief (e.g., Ebert et al. 2012, Hall et al. 2013). The initial data collection from TPI therefore performs at a higher level on sedimentary bedrock, where glacial erosion has a higher impact on bedform slope, than across crystalline bedrock where glacial erosion is less effective at deforming the surface. False positive TPI bedforms have no correlation

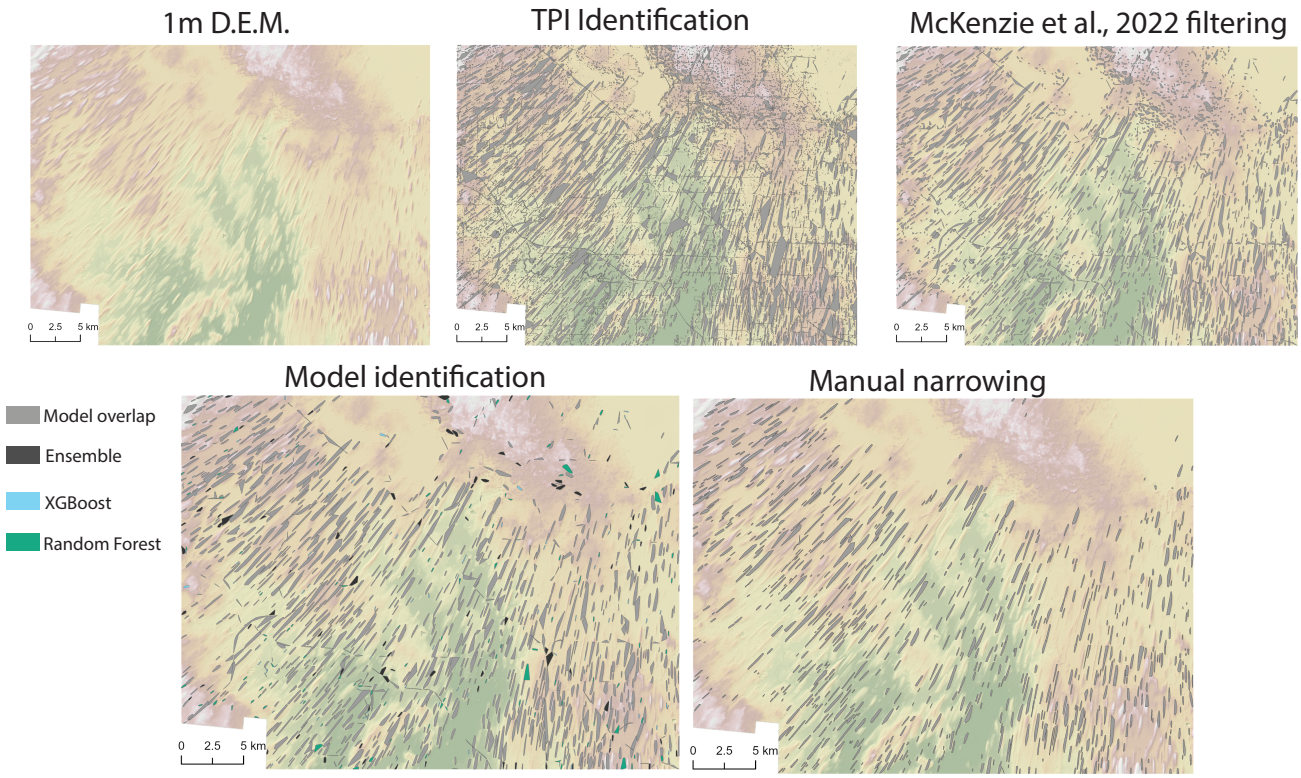

FIGURE 5 Spatial representation of model performance. Panels include ambient occlusion techniques performed on a set of 1 meter DEMs from USGS 3DEM. Positive relief features identified by TPI identification are represented by gray polygons. The original TPI dataset underwent scientifically-based filtering using reasoning from McKenzie et al. (2022). The filtered dataset underwent Random Forest, XGBoost, and Ensemble Average model analysis. Significant spatial overlap in the model identification is indicated by gray polygons in the lower left map panel. Manual identification from TPI identified features was used to ground-truth the model performance and used to develop curves in Figure 4.

to site topography or lithology (McKenzie et al. 2022). Additional information about limitations of TPI identification can be found within the discussion of McKenzie et al. (2022).

In this work, we identify the topographic and lithologic conditions of each site into either a topographically "open" or "closed" system and either a "sedimentary" or "crystalline/volcanic" bedrock. Nuances between individual erosional or depositional features, variation in types of sedimentary or crystalline bedrock, or topographic complexity across a single site was therefore not captured in the training dataset. However, this binary classification of topography and lithology act as a strength in this work. The only necessary input from users to quantitatively analyze deglaciated regions are general bedrock lithology classifications, regional topographic constraints, and elevation data. Nuances in bedform type, implicit to bedform morphometrics, may be lost in this approach but generalizing our classification system allows for a globalization of bedform identification. Secondary analyses after automated bedform identification can reincorporate data specificity and consider the complexity between bedform characteristics, formation, and location.

The training dataset includes four sites with open topography and sedimentary bedrock, two sites with topographic constraints and crystalline bedrock, two sites with open topography and crystalline bedrock, and one site with topographic constraints and sedimentary bedrock 1. The choice of sites for the training dataset limits the model's ability to extrapolate results to new regions with topographic constraints or bedrock type that are out-of-distribution (OOD). Any applications of the tools in this paper to OOD data are statistically unreliable but will still provide a starting point to analyzing presence of streamlined subglacial bedforms across a deglaciated landscape. Section 2.3.3 provides an example of successful application to an OOD region. Future incorporation of streamlined subglacial bedform data across a variety of bed conditions into the training dataset will improve the model's ability to predict the origin of other positive relief features in new locations.

In order to maintain as much generalizability as possible to new regions that share similar topographic constraints (open or closed) and similar bedrock features (sedimentary or crystalline/volcanic), we implemented a filtering schema that incorporates scientific decision making in the preprocessing of our training set. A filtering process focused on likelihood of streamlined subglacial bedform morphometrics is generally

reproducible in new sites, even where the glacial bedforms are not yet known, as it filters candidate landforms on observable characteristics such as length, width, and orientation. In contrast, a purely statistical downsampling approach, such as Near Miss, when implemented without a scientifically driven modulation, is unable to be reproduced unless "true" bedforms from manual identification are already known and overfits to the training data. This leads to a less flexible model fit downstream that would strongly underpredict bedforms in a new area, highlighting the importance of incorporating scientifically driven decision making into the ML pipeline.

3.3 | Validating Trends with Feature Importance

The four input features used by the ML models to determine which positive relief features are streamlined subglacial bedforms include feature area, elongation, site topography (open or constrained), and site lithology (crystalline/volcanic or sedimentary). The relative strength of a particular feature in determining the accuracy of the final predictions can be measured in both Random Forest and XGBoost. This measure is called "feature importance," and we show the relative contributions of the input features in Figure 6a. The area and elongation of a positive relief feature are the most influential in determining whether or not a feature is a streamlined subglacial bedform. Bedform area and elongation are values unique to each feature and are inherently related to formation process based on continuum properties of streamlined subglacial bedforms (e.g., Ottesen and Dowdeswell 2006, Stokes and Clark 2002).

The topography and bed lithology values assigned to each bedform are integrated across sites within the training dataset. This generalization therefore contributes to topography and bed lithology as being the two least important factors contributing to the model's determination of whether or not a feature is a streamlined subglacial bedform. However, is is important to note that site topography is listed as a higher order control on bedform determination than bed lithology. Ice streaming behavior, therefore, is less affected by bed lithology than topography. Whereas this has been well-established in literature comparing ice streaming behavior across various sites (e.g., Greenwood and Clark 2010, Greenwood et al. 2021, McKenzie et al. 2022), statistically confirming this importance (Figure 6a) in two distinct ML models further supports this hypothesis in landscape analysis.

In observing the point data from the training dataset, Figure 6b highlights that while streaming occurs across a continuum of length to width values for individual bedforms, streamlined subglacial bedforms observed at sites with unconstrained topography typically have smaller width and length values than bedforms observed at site within constrained topographic systems. A similar relationship does not stand for streamlined subglacial bedforms between sites of similar bed lithology, further supporting the inference from the importance contribution values that topography is more influential to determining ice streaming than bed lithology. Furthermore, we note that all topographic and lithologic bedform subtypes create similar bimodal distributions except for bedforms identified on the sedimentary bedrock and closed topography of the Puget Lowland, as is shown in the marginal distributions of Figure 6b. The bimodal distribution of datapoints at all sites other than the sedimentary bed and closed topography likely points to a continuum of bedform development in glacial streaming: where pressure differences at the ice bed (Jauhiainen 1975), variations in individual bedform composition and resistance to erosion (Menzies 1979), and maturity of the streamlined subglacial feature (Benediktsson et al. 2016) all contribute to a continuum of bedform morphologies (Ely et al. 2016) with a bimodal distribution (Figure 6b). This co-development of the range of bedform morphologies is also apparent in the spatial distribution of elongation seen in McKenzie et al. (2022). Conversely, the sedimentary region with closed topography of the Puget Lowland appears to primarily display higher values of bedform width and length, indicating a distinct similarity in bedform composition (Menzies 1979) and more sustained streaming Benediktsson et al. (2016), with relatively little representation of shorter, narrower bedforms.

3.4 | Reanalysis of a subset of Green Bay Lobe bedforms

In applying `bedmap` to the Green Bay Lobe, all three models automatically identified 1,073 streamlined subglacial bedforms. In this overlapping dataset, we identify the average elongation of the features as 7.83 and the average orientation of streamlined subglacial bedform long axis as 41.44 cardinal degrees. These results provide additional evidence that builds upon previous work in this region that have identified streaming conditions (Colgan and Mickelson 1997), basal drag flux (Zoet et al. 2021), and bed roughness (Eyles et al. 2022) of the larger Green Bay Lobe. With minimal manual effort, we have robustly derived general ice flow direction and streamlined subglacial bedform elongation of this subregion of Green Bay Lobe flow with a larger number of streamlined subglacial bedforms and the associated quantitative data.

As the Wisconsin Green Bay Lobe site was the first OOD application of `bedmap`, we contrast the detections with manual identification. Of all identified bedforms, 24% of the Random Forest bedforms, 22% of the XGBoost bedforms, and 20% of the Ensemble Average bedforms were false positives (i.e., positive relief features identified as streamlined subglacial bedforms that are not). These false positive features are primarily landforms representing the edge of roads and some river banks. The Random Forest model identified false positives on fragmented streamlined subglacial bedforms or on positive relief features that expanded beyond the area of a true streamlined subglacial bedform (Figure A1). XGBoost identified false positives among positive relief features with smaller areas and smaller widths than any of the other model-identified false positives. The incorrectly identified features include fragmented streamlined subglacial bedforms and road-edges. It should be noted that upon closer assessment, the Random Forest and XGBoost models identified streamlined subglacial bedforms that had originally been missed

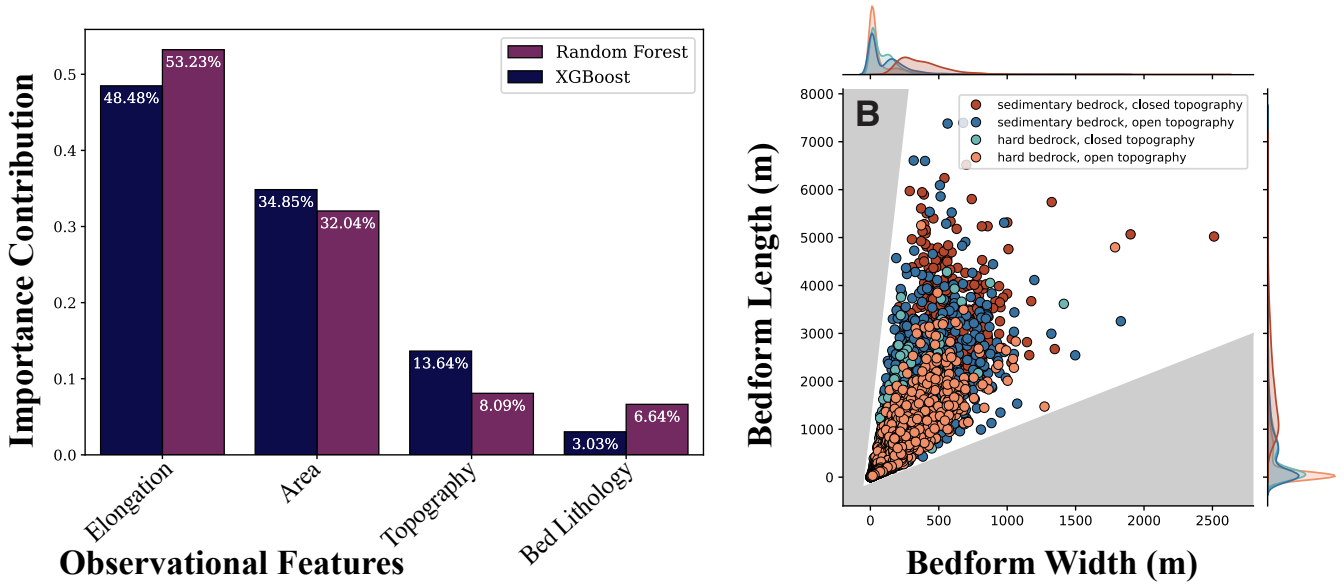

FIGURE 6 A) Relative contributions of input features to prediction outcomes in the Random Forest and XGBoost models. Positive relief area and elongation together contribute to $> 80\%$ of the learned outcome in both models, but it is clear that non-geometric geomorphological features like topography and bed lithology further contextualize to the model's understanding. B) The length/width distribution of glacially-derived bedform features, distinguished in color by bed lithology and topography. Marginal distributions are shown for each axis, indicating similar distributions for all lithological and topographical combinations except for the site that has a sedimentary bed and closed topography.

in manual assessment, highlighting the utility of these tools in providing a useful guideline for mapping of streamlined subglacial bedforms (see Figure A1). Streamlined subglacial bedforms that were manually identified from the TPI dataset and missed by all models have smaller areas than the majority of the bedforms identified by the ML approach. The model may have missed some of the smaller streamlined subglacial bedforms due to the statistical likelihood that the majority of smaller features are not bedforms. `bedmap`'s ability to identify smaller streamlined subglacial bedforms can be improved in future versions by incorporating more training data that includes these smaller features, thereby enhancing its capacity to detect a broader spectrum of new data.

While Random Forest outperformed the XGBoost and Ensemble Average models in the cross-validation runs, in this OOD region, XGBoost outperformed the Random Forest and Ensemble Average models (Figure 4). Although XGBoost and Random Forest both deliver top performance at times, the Ensemble Average model consistently delivers a performance that closely approximates the top-performing model in both cases. With this in mind, especially when applying the models to sites without manual comparisons, the Ensemble Average model run will be the safest run to receive accurate results.

3.5 | Future directions for tool advancements

Data standards and metadata used to share glacial geomorphology data are highly variable due to a range in the interests for mapping deglaciated landscapes (Chandler et al. 2018). Typically, the purpose of data collection influences how decisions are made about metadata and data sharing. The history of streamlined subglacial bedform identification in the field of glacial geomorphology has resulted in an incredible number of glacial feature datasets that support the ability to interpret entire ice sheet histories from bedform assemblages, build understanding of processes that control bedform formation and evolution, contribute to identifying glaciation style, identify areas of interest for field campaigns, and provide constraints to ice sheet modeling (Chandler et al. 2018). Streamlined subglacial bedforms have been mapped using a wide range of techniques (e.g., Principato et al. 2016, Norris et al. 2017, Spagnolo et al. 2017, Wang et al. 2017, Saha et al. 2011, Sookhan et al. 2021, Eyles et al. 2022, McKenzie et al. 2022). While all of these methods contribute necessary knowledge to the field, each dataset is subject to varied levels of manual input and scalability has proven difficult in an era where there is unprecedented data availability. Furthermore, variations in manual classification choices from expert to expert can lead to subjective and difficult to reproduce classification schema with associated unquantified error.

Several efforts in the last few years have focused on using previous work to develop a single map of glacial features across Britain (BRITICE: Clark et al. 2018), the Arctic (GlaciDat: Streuff et al. 2022), and Greenland[](Leger et al. 2024) Even so, it is not yet always customary to make developed mapping tools and geomorphic datasets from deglaciated landscapes fully open and publicly available. There is an importance for geoscientific data, including geomorphic analyses, to meet FAIR data

standards (Wilkinson et al. 2016) as recommended by NASA's Transform to Open Science Initiative (Gentemann 2023) and emphasized at NCAR's recent "Community Expectations for a Geoscience Data Commons" workshop, which had wide international representation. Many previously developed datasets meet some or all of these standards (e.g., Clark et al. 2018, Streuff et al. 2022, Norris et al. 2017, Greenwood et al. 2021, McKenzie et al. 2022 2023). In order for geomorphological concepts and data related to subglacial processes to be incorporated into models of modern glacial systems and transferable for ML efforts in the glacial geomorphology sphere, it is imperative that FAIR data sharing are made commonplace. Further, the glacial geochronology community has taken steps toward making previously published data open and widely accessible through the establishment of the Informal Cosmogenic-nuclide Exposure-age Database (ICE-D) (Balco 2020). When tools for open and FAIR geomorphic datasets are paired with data from ICE-D, we will have a powerful tool for establishing ice histories across large spatial scales (e.g., Leger et al. 2024, Stoker et al. 2024).

Automating mapping efforts with the use of ML is a natural next step to further progress and efficiency within the field of glacial geomorphology. The use of a quantifiable and reproducible classification model enables the comparison of large datasets across vast spatial scales while maintaining a statistically robust comparison. ML approaches in glacial geomorphology can enable us to further elucidate controlling factors of subglacial conditions on basal regimes and ice streaming, both by providing further confirmations of existing hypotheses, such as we showcased in Section 3.3, and by reducing the amount of time and effort necessary to calculate secondary data products as we highlighted in Section 3.4. By using much of the mapping that has been manually verified and made publicly available (e.g., Clark et al. 2018, Norris et al. 2017, Greenwood et al. 2021, Streuff et al. 2022, McKenzie et al. 2022 2023), ML tools will be greatly improved and increase accessibility of mapping efforts to the broader scientific community.

4 | CONCLUSIONS

In previous studies, manual and variations of semi-automatic identification of glacially derived bedforms across deglaciated landscapes proved to be time-consuming and prone to human error. To address this, we introduce a supervised machine learning approach that automates the identification of streamlined subglacial bedforms. Utilizing Random Forest, XGBoost, and an Ensemble Average models, trained on a comprehensive dataset spanning nine sites across the deglaciated Northern Hemisphere with robust verification, we created an open source Python package that can be used on ArcGIS outputs to robustly automate detection of bedforms from TPI products in minutes. Our approach demonstrates high accuracy and stability, achieving true positive detection rates of up to 94.5%.

The generalizability of `bedmap` enables seamless application to datasets in new regions, which we illustrate by applying our workflow to a new DEM in the Green Bay Lobe region. Using the combination of TPI and `bedmap`, we identify the average elongation of features as 7.83 and the average orientation of the subglacial bedform long axis as 41.44 cardinal degrees in this region. In a workflow that relies on manual identification, the derivation of general ice flow and direction from a DEM across large areas could take over tens of hours, but with `bedmap` it is achieved in a matter of minutes. Futhermore, our efficient method contributes to minimizing human-induced errors in the final streamlined subglacial bedform dataset, advancing the field of glacial geomorphology through open science practices and machine learning innovation.

DATA AVAILABILITY

In addition to the training dataset and Python codes for this tool made available through Zenodo and CryoCloud, a Jupyter Book is being developed for step-by-step instructions on tool execution. The Zenodo-published Jupyter Book will include chapters such as "Uploading geomorphology data into Python" and "Training a Random Forest tool". The training dataset and TPI tool is available from McKenzie et al., 2022.

AUTHOR CONTRIBUTIONS

E. Abrahams is responsible for project conception, analysis, data and code production, initial writing, editing, and visualization. M. McKenzie is responsible for project conception, data collection, analysis, data and code production, initial writing, editing, and visualization. F. Pérez is responsible for editing and code editing. R. Venturelli is responsible for project conception and editing.

ACKNOWLEDGMENTS

Testing and development of this paper was done on the CryoCloud cloud-based JupyterHub (Snow et al. 2023) that is funded by the NASA Transform to Open Science Program and ICESat-2 Science Team (grant numbers 80NSSC23K0002 and 80NSSC22K1877). The authors would like to acknowledge NSF EAR Postdoctoral Grant 2305317 for supporting M. McKenzie in development of this work. EA gratefully acknowledges support from a Two Sigma PhD Fellowship.

This work was developed and written on land historically inhabited by the Arapahoe, Lipan Apache, Cheyenne, Ho-Chunk, Skokomish, Suquamish, Squaxin, Stl'pulmsh, Steilacoom, Puyallup, Muckleshoot, Duwamish, Cree, Eeyou Istchee, Innu, Sámi, Erie, Kaskaskia, xučyun (Chochenyo speaking Muwekma Ohlone peoples), and Ramaytush Ohlone peoples, custodians of the land time immemorial. The authors respect these people's sovereignty and stewardship of the land past, present, and future. We have benefited, and continue to benefit, from the use of this land. We recognize the importance of taking actions in support of American Indian and Indigenous peoples who are living, flourishing members of our communities today.

FINANCIAL DISCLOSURE

None reported.

CONFLICT OF INTEREST

The authors declare no potential conflict of interests.

REFERENCES

Abrahams, E., Snow, T., Siegfried, M.R. & Pérez, F. (2024) *A Concise Tiling Strategy for Preserving Spatial Context in Earth Observation Imagery*.

Ali, N., Chen, J., Fu, X., Ali, R., Hussain, M.A., Daud, H. et al. (2024) Integrating Machine Learning Ensembles for Landslide Susceptibility Mapping in Northern Pakistan. *Remote Sensing*, 16, 988. doi:10.3390/rs16060988.

Balco, G. (2020) Technical note: A prototype transparent-middle-layer data management and analysis infrastructure for cosmogenic-nuclide exposure dating. *Geochronology*, 2(2), 169–175. doi:10.5194/gchron-2-169-2020.

Benediktsson, Í.Ö., Jónsson, S.A., Schomacker, A., Johnson, M.D., Ingólfsson, Ó., Zoet, L. et al. (2016) Progressive formation of modern drumlins at Múlajökull, Iceland: Stratigraphical and morphological evidence. *Boreas*, 45(4), 567–583. doi:10.1111/bor.12195.

Boulton, G.S. (1976) The Origin of Glacially Fluted Surfaces-Observations and Theory. *Journal of Glaciology*, 17(76), 287–309. doi:10.3189/S0022143000013605.

Breiman, L. (2001) Random Forest. *Machine Learning*, 45(1), 5–32. doi:10.1023/A:1010933404324.

Chandler, B.M.P., Lovell, H., Boston, C.M., Lukas, S., Barr, I.D., Benediktsson, Í.Ö. et al. (2018) Glacial geomorphological mapping: A review of approaches and frameworks for best practice. *Earth-Science Reviews*, 185, 806–846. doi:10.1016/j.earscirev.2018.07.015.

Chen, T. & Guestrin, C. XGBoost: A Scalable Tree Boosting System. In: *Proceedings of the 22nd ACM SIGKDD International Conference on Knowledge Discovery and Data Mining. KDD '16, Aug. 2016*. New York, NY, USA: Association for Computing Machinery, pp. 785–794.

Clark, C.D., Ely, J.C., Greenwood, S.L., Hughes, A.L.C., Meehan, R., Barr, I.D. et al. (2018) BRITICE Glacial Map, version 2: A map and GIS database of glacial landforms of the last British–Irish Ice Sheet. *Boreas*, 47(1), 11. doi:10.1111/bor.12273.

Colgan, P.M. & Mickelson, D.M. (1997) Genesis of streamlined landforms and flow history of the Green Bay Lobe, Wisconsin, USA. *Sedimentary Geology*, 111(1-4), 7–25. doi:10.1016/S0037-0738(97)00003-1.

Ebert, K., Hall, A. & Hättestrand (2012) Pre-glacial landforms on a glaciated shield: The inselberg plains of northern Sweden. *Norwegian Journal of Geology*,(92), 1–18.

Ely, J.C., Clark, C.D., Spagnolo, M., Stokes, C.R., Greenwood, S.L., Hughes, A.L.C. et al. (2016) Do subglacial bedforms comprise a size and shape continuum? *Geomorphology*, 257, 108–119. doi:10.1016/j.geomorph.2016.01.001.

Eyles, N., Arbelaez Moreno, L. & Sookhan, S. (2018) Ice streams of the Late Wisconsin Cordilleran Ice Sheet in western North America. *Quaternary Science Reviews*, 179, 87–122. doi:10.1016/j.quascirev.2017.10.027.

Eyles, N., Bukhari, S., Sookhan, S., Ruscica, P. & Paulen, R. (2022) LiDAR-based semi-automated mapping of drumlins and mega-scale glacial lineations of the Green Bay Lobe, Wisconsin, USA: Ice sheet beds as glaciotribological systems. *Earth Surface Processes and Landforms*, 48(2), 295–321. doi:10.1002/esp.5486.

Flach, P.A. & Kull, M. Precision-Recall-Gain curves: PR analysis done right. In: *Proceedings of the 28th International Conference on Neural Information Processing Systems - Volume 1. NIPS'15, Dec. 2015*. Cambridge, MA, USA: MIT Press, pp. 838–846.

Geisser, S. (2019) *Predictive Inference*. New York: Chapman and Hall/CRC.

Gentemann, C. (2023) Why NASA and federal agencies are declaring this the Year of Open Science. *Nature*, 613(7943), 217–217. doi:10.1038/d41586-023-00019-y.

Graham, A.G., Larter, R.D., Gohl, K., Hillenbrand, C.D., Smith, J.A. & Kuhn, G. (2009) Bedform signature of a West Antarctic palaeo-ice stream reveals a multi-temporal record of flow and substrate control. *Quaternary Science Reviews*, 28(25-26), 2774–2793. doi:10.1016/j.quascirev.2009.07.003.

Granger, B.E. & Pérez, F. (2021) Jupyter: Thinking and Storytelling With Code and Data. *Computing in Science & Engineering*, 23(2), 7–14. doi:10.1109/MCSE.2021.3059263.

Greenwood, S.L. & Clark, C.D. (2010) The sensitivity of subglacial bedform size and distribution to substrate lithological control. *Sedimentary Geology*, 232(3-4), 130–144. doi:10.1016/j.sedgeo.2010.01.009.

Greenwood, S.L., Simkins, L.M., Winsborrow, M.C.M. & Bjarnadóttir, L.R. (2021) Exceptions to bed-controlled ice sheet flow and retreat from glaciated continental margins worldwide. *Science Advances*, 7(3), eabb6291. doi:10.1126/sciadv.abb6291.

Hall, A.M., Ebert, K. & Hättestrand, C. (2013) Pre-glacial landform inheritance in a glaciated shield landscape. *Geografiska Annaler: Series A, Physical Geography*, 95(1), 33–49. doi:10.1111/j.1468-0459.2012.00477.x.

Holschuh, N., Christianson, K., Paden, J., Alley, R. & Anandakrishnan, S. (2020) Linking postglacial landscapes to glacier dynamics using swath radar at Thwaites Glacier, Antarctica. *Geology*, 48(3), 268–272. doi:10.1130/G46772.1.

Hughes, A.L., Clark, C.D. & Jordan, C.J. (2010) Subglacial bedforms of the last British Ice Sheet. *Journal of Maps*, 6(1), 543–563. doi:10.4113/jom.2010.1111.

James, G., Witten, D., Hastie, T., Tibshirani, R. & Taylor, J. (2023) *An Introduction to Statistical Learning: With Applications in Python*. Springer Texts in Statistics. Cham: Springer International Publishing.

Jauhiainen, E. (1975) Morphometric analysis of drumlin fields in northern Central Europe. *Boreas*, 4, 219–230.

King, E.C., Hindmarsh, R.C.A. & Stokes, C.R. (2009) Formation of mega-scale glacial lineations observed beneath a West Antarctic ice stream. *Nature Geoscience*, 2(8), 585–588. doi:10.1038/ngeo581.

Leger, T.P.M., Clark, C.D., Huynh, C., Jones, S., Ely, J.C., Bradley, S.L. et al. (2024) A Greenland-wide empirical reconstruction of paleo ice sheet retreat informed by ice extent markers: PaleoGrIS version 1.0. *Climate of the Past*, 20(3), 701–755. doi:10.5194/cp-20-701-2024.

Li, J., Zhang, H., Zhao, J., Guo, X., Rihan, W. & Deng, G. (2022) Embedded Feature Selection and Machine Learning Methods for Flash Flood Susceptibility-Mapping in the Mainstream Songhua River Basin, China. *Remote Sensing*, 14, 5523. doi:10.3390/rs14215523.

Mani, I. & Zhang, I. kNN approach to unbalanced data distributions: A case study involving information extraction. In: *Proceedings of Workshop on Learning from Imbalanced Datasets*. Vol. 126, *2003*. : International Conference on Machine Learning, pp. 1–7.

McKenzie, M.A., Miller, L.E., Slawson, J.S., MacKie, E.J. & Wang, S. (2023) Differential impact of isolated topographic bumps on ice sheet flow and subglacial processes. *The Cryosphere*, 17(6), 2477–2486. doi:10.5194/tc-17-2477-2023.

McKenzie, M.A., Simkins, L.M., Principato, S.M. & Munevar Garcia, S. (2022) Streamlined subglacial bedform sensitivity to bed characteristics across the deglaciated Northern Hemisphere. *Earth Surface Processes and Landforms*, 47(9), 2341–2356. doi:10.1002/esp.5382.

Menzies, J. (1979) A review of the literature on the formation and location of drumlins. *Earth Science Reviews*, 14, 315–359.

More, A.S. & Rana, D.P. Review of random forest classification techniques to resolve data imbalance. In: *2017 1st International Conference on Intelligent Systems and Information Management (ICISIM), Oct. 2017*. Aurangabad: IEEE, pp. 72–78.

Mudrey, Jr., M., Brown, B. & Greenberg, J. (1982) *Bedrock Geologic Map of Wisconsin*.

Norris, S.L., Margold, M. & Froese, D.G. (2017) Glacial landforms of northwest Saskatchewan. *Journal of Maps*, 13(2), 600–607. doi:10.1080/17445647.2017.1342212.
Ottesen, D. & Dowdeswell, J.A. (2006) Assemblages of submarine landforms produced by tidewater glaciers in Svalbard. *Journal of Geophysical Research: Earth Surface*, 111(F1), 2005JF000330. doi:10.1029/2005JF000330.
Pedregosa, F., Varoquaux, G., Gramfort, A., Michel, V., Thirion, B., Grisel, O. et al. (2011) Scikit-learn: Machine learning in Python. *Journal of Machine Learning Research*, 12, 2825–2830.
Pérez, F., Granger, B.E. & Hunter, J.D. (2011) Python: An Ecosystem for Scientific Computing. *Computing in Science & Engineering*, 13(2), 13–21. doi:10.1109/MCSE.2010.119.
Principato, S.M., Moyer, A.N., Hampsch, A.G. & Ipsen, H.A. (2016) Using GIS and streamlined landforms to interpret palaeo-ice flow in northern Iceland. *Boreas*, 45(3), 470–482. doi:10.1111/bor.12164.
Prothro, L.O., Simkins, L.M., Majewski, W. & Anderson, J.B. (2018) Glacial retreat patterns and processes determined from integrated sedimentology and geomorphology records. *Marine Geology*, 395, 104–119. doi:10.1016/j.margeo.2017.09.012.
Rezvani, S. & Wang, X. (2023) A broad review on class imbalance learning techniques. *Applied Soft Computing*, 143, 110415. doi:10.1016/j.asoc.2023.110415.
Roberts, D.H. & Long, A.J. (2005) Streamlined bedrock terrain and fast ice flow, Jakobshavns Isbrae, West Greenland: Implications for ice stream and ice sheet dynamics. *Boreas*, 34(1), 25–42. doi:10.1080/03009480510012818.
Saha, K., Wells, N.A. & Munro-Stasiuk, M. (2011) An object-oriented approach to automated landform mapping: A case study of drumlins. *Computers & Geosciences*, 37(9), 1324–1336. doi:10.1016/j.cageo.2011.04.001.
Simkins, L.M., Greenwood, S.L. & Anderson, J.B. (2018) Diagnosing ice sheet grounding line stability from landform morphology. *The Cryosphere*, 12(8), 2707–2726. doi:10.5194/tc-12-2707-2018.
Snow, T., Millstein, J., Scheick, J., Sauthoff, W., Leong, W.J., Colliander, J. et al. (2023) *CryoCloud JupyterBook*. Zenodo.
Sookhan, S., Eyles, N., Bukhari, S. & Paulen, R.C. (2021) LiDAR-based quantitative assessment of drumlin to mega-scale glacial lineation continuums and flow of the paleo Seneca-Cayuga paleo-ice stream. *Quaternary Science Reviews*, 263, 107003. doi:10.1016/j.quascirev.2021.107003.
Spagnolo, M., Bartholomaus, T.C., Clark, C.D., Stokes, C.R., Atkinson, N., Dowdeswell, J.A. et al. (2017) The periodic topography of ice stream beds: Insights from the Fourier spectra of mega-scale glacial lineations. *Journal of Geophysical Research: Earth Surface*, 122(7), 1355–1373. doi:10.1002/2016JF004154.
Spagnolo, M., Clark, C.D., Ely, J.C., Stokes, C.R., Anderson, J.B., Andreassen, K. et al. (2014) Size, shape and spatial arrangement of mega-scale glacial lineations from a large and diverse dataset. *Earth Surface Processes and Landforms*, 39(11), 1432–1448. doi:10.1002/esp.3532.
Stoker, B.J., Dulfer, H.E., Stokes, C.R., Brown, V.H., Clark, C.D., Ó Cofaigh, C. et al. (2024) *Ice flow dynamics of the northwestern Laurentide Ice Sheet during the last deglaciation*.
Stokes, C., Spagnolo, M., Clark, C., Ó Cofaigh, C., Lian, O. & Dunstone, R. (2013) Formation of mega-scale glacial lineations on the Dubawnt Lake Ice Stream bed: 1. size, shape and spacing from a large remote sensing dataset. *Quaternary Science Reviews*, 77, 190–209. doi:10.1016/j.quascirev.2013.06.003.
Stokes, C.R. & Clark, C.D. (2002) Are long subglacial bedforms indicative of fast ice flow? *Boreas*, 31(3), 239–249. doi:10.1111/j.1502-3885.2002.tb01070.x.
Stokes, C.R., Margold, M. & Creyts, T.T. (2016) Ribbed bedforms on palaeo-ice stream beds resemble regular patterns of basal shear stress ('traction ribs') inferred from modern ice streams. *Journal of Glaciology*, 62(234), 696–713. doi:10.1017/jog.2016.63.
Streuff, K.T., Ó Cofaigh, C. & Wintersteller, P. (2022) GlaciDat – a GIS database of submarine glacial landforms and sediments in the Arctic. *Boreas*, 51(3), 517–531. doi:10.1111/bor.12577.
Ting, K.M. (2011) Confusion Matrix. In: Sammut, C. & Webb, G.I. (Eds.) *Encyclopedia of Machine Learning*. Boston, MASpringer US, pp. 209–209.
Wang, S., Wu, Q. & Ward, D. (2017) Automated delineation and characterization of drumlins using a localized contour tree approach. *International Journal of Applied Earth Observation and Geoinformation*, 62, 144–156. doi:10.1016/j.jag.2017.06.006.
Wilkinson, M.D., Dumontier, M., Aalbersberg, I.J., Appleton, G., Axton, M., Baak, A. et al. (2016) The FAIR Guiding Principles for scientific data management and stewardship. *Scientific Data*, 3(1), 160018. doi:10.1038/sdata.2016.18.
Zhao, Z. & Chen, J. (2023) A robust discretization method of factor screening for landslide susceptibility mapping using convolution neural network, random forest, and logistic regression models. *International Journal of Digital Earth*, 16, 408–429. doi:10.1080/17538947.2023.2174192.
Zoet, L.K., Rawling, J.E., Woodard, J.B., Barrette, N. & Mickelson, D.M. (2021) Factors that contribute to the elongation of drumlins beneath the Green Bay Lobe, Laurentide Ice Sheet. *Earth Surface Processes and Landforms*, 46(13), 2540–2550. doi:10.1002/esp.5192.

SUPPORTING INFORMATION

Additional supporting information may be found in the online version of the article at the publisher's website.

How to cite this article: Abrahams E, McKenzie M, Pérez F, and Venturelli R. Automatic identification of subglacial streamlined bedforms using machine learning *Boreas*

APPENDIX

A FINDING THE BEST MODEL FIT

A.1 Explanation of Performance Metrics

Performance metrics serve as critical evaluation measures for assessing the efficacy of a model fit. These metrics provide quantifiable measures of how well a model aligns with the observed data, offering insights into the robusticity of a model's predictive capabilities and generalization potential to new data. These metrics look at the relationships between true positives (in our case, when the model correctly detects a bedform), true negatives (when the model correctly detects that a landform is not a bedform), false positives (when the model mistakes another landform for a bedform), and false negatives (when the model misses detecting a bedform).

Accuracy (Equation A1) is one of the a commonly used metric in the evaluation Earth Science classification tasks, and quantifies the proportion of correctly classified detections to the total number of predictions. In the case of balanced classification, accuracy is a concise measure of overall predictive correctness, however when applied to cases of class imbalance like the one in this paper, accuracy is dominated by the larger class (in our case true negatives), and does not fully capture where such

a model might fail in detecting true positives. We include the accuracy score in this paper to maintain continuity with standard practices in the field of spatial statistics.

$$\text{Accuracy} = \frac{\text{True Positives + True Negatives}}{\text{Total Number of Predictions}} \tag{A1}$$

Precision (Equation A2) quantifies how often a classification model correctly predicts the positive class. In other words, precision focuses on the accuracy of the model's positive predictions, rather than its ability to detect all potential instances. High precision indicates a low rate of false positives.

$$\text{Precision} = \frac{\text{True Positives}}{\text{True Positives + False Positives}} \tag{A2}$$

In contrast, recall (Equation A3) measures the models ability to correctly identify all instances of positive predictions. Specifically, recall calculates the proportion of true positives to all the instances that truly belong to the positive class. High recall indicates a low rate of false negatives.

$$\text{Recall} = \frac{\text{True Positives}}{\text{True Positives + False Negatives}} \tag{A3}$$

Since recall and precision are both important measures in the case of class imbalance, where it is easier for a model to miss and mistake positive instances, the F1 score (Equation A4) combines precision and recall into a single measure, considering both false positives and false negatives. The F1 score prevents an overly optimistic assessment that can occur when only focusing on recall or precision, and provides a score that is balanced towards a low rate of false positives and false negatives. In the McKenzie et al. (2022) filtered data, bedforms make up just under 20% of all observations. For this reason, we primarily focus on F1 score throughout this work.

$$\begin{aligned}\text{F1 Score} &= 2 \times \frac{\text{Precision} \times \text{Recall}}{\text{Precision} + \text{Recall}} \\ &= 2 \times \frac{\text{True Positives}}{\text{True Positives} + \text{False Positives} + \text{False Negatives}}\end{aligned} \tag{A4}$$

We calculate all performance scores using the `scikit-learn` library in Python. We share the implementation of these calculations in the supplementary Jupyter Book. See Flach and Kull (2015) for an overview of the limitations of these metrics.

A.2 Cross Validation Grid Search for Random Forest and XGBoost

In order to develop robust and accurate predictive models for identifying glacially derived streamlined features, we conducted extensive cross-validation grid searches to optimize the hyperparameters of both Random Forest and XGBoost models. Hyperparameters are essential settings that govern the behavior of machine learning algorithms and directly impact model performance. By systematically exploring different combinations of hyperparameters, we aimed to identify the configurations that maximize the models' predictive capabilities while minimizing overfitting.

For the Random Forest model, the grid search spanned several key hyperparameters, including Maximum Features, Minimum Samples per Leaf, Minimum Samples per Split, and Number of Estimators. Maximum Features determines the maximum number of features considered for splitting at each tree node, while Minimum Samples per Leaf and Minimum Samples per Split control the minimum number of samples required to be present in a leaf node and the minimum number of samples required to split an internal node, respectively. Additionally, Number of Estimators specifies the number of trees in the forest. By exploring various combinations of these hyperparameters, we sought to identify the configuration that yields the optimal balance between model complexity and predictive performance.

Similarly, for the XGBoost model, the grid search encompassed a broader range of hyperparameters, including Maximum Depth, Minimum Child Weight, Gamma, Subsample, Column Subsampling Rate, Learning Rate, and Number of Estimators. Maximum Depth controls the maximum depth of each tree in the ensemble, while Minimum Child Weight specifies the minimum sum of instance weights required to create a new child node. Gamma determines the minimum loss reduction required to make a further partition on a leaf node, providing a regularization mechanism to prevent overfitting. Subsample and Column Subsampling Rate regulate the subsampling of training instances and columns when constructing each tree, contributing to improved generalization. Learning Rate shrinks the contribution of each tree during training, preventing overfitting, while Number of Estimators sets the number of boosting rounds.

Table A1 presents the cross-validation grid searches for both Random Forest and XGBoost models, showcasing the combinations of hyperparameters tested. By systematically evaluating these hyperparameter configurations, we identified the optimal settings for our predictive Random Forest and XGBoost models, ultimately enhancing their accuracy and robustness in identifying new glacially derived streamlined features across diverse landscapes and regions.

A.3 Spatial validation of model performance

We show the contrast between the estimated model outcomes of shapefile output in the Wisconsin Green Bay Lobe. Figure A1 shows the overlap between all three models, and examples of how each model creates a small percentage of mistaken features. We also show how the models can detect streamlined subglacial bedforms that were previously missed in manual identification.

TABLE A1 Cross validation grid for optimal hyperparameter search. Both searches were conducted using `scikit-learn`'s custom cross-validation function so that the models were trained on data filtered both with McKenzie et al. (2022) filtering and Near Miss, but validated on data filtered only with McKenzie et al. (2022) filtering

Random Forest Cross Validation Grid	
Hyperparameter	Grid
`min_samples_leaf`	2, 5, 10
`min_samples_split`	50, 100, 150, 250
`n_estimators`	25, 50, 100, 500, 1000
XGBoost Cross Validation Grid	
Hyperparameter	Grid
`max_depth`	3, 5, 7, 9
`min_child_weight`	1, 5, 10
`gamma`	0.0, 0.1, 0.25, 0.5, 1.0
`subsample`	0.4, 0.5, 0.6
`colsample_bytree`	0.5, 0.6, 0.75, 1.0
`learning_rate`	0.01, 0.1, 0.15
`n_estimators`	10, 50, 100, 200

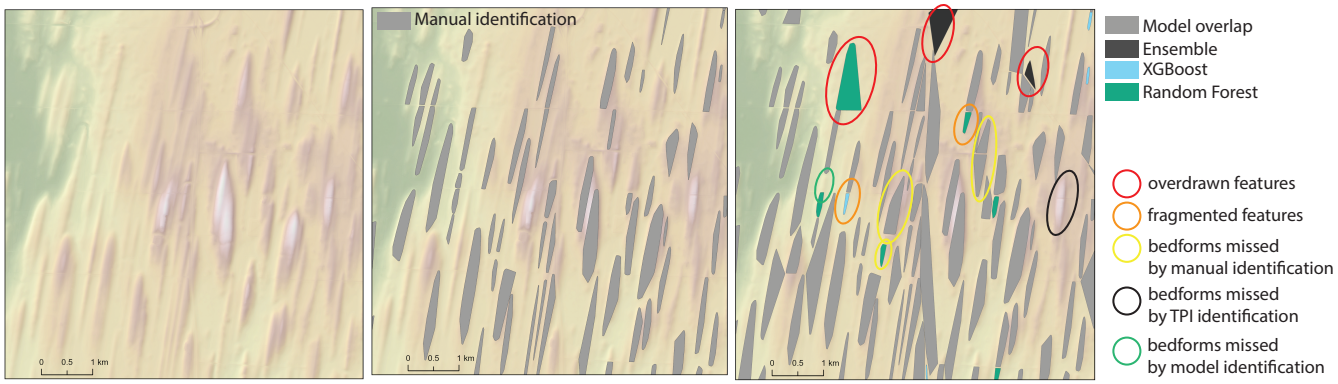

FIGURE A1 Example of manual identification of streamlined subglacial bedforms in comparison to model output. There are examples of feature boundaries outside of true bedform perimeters (overfit), fragmented streamlined subglacial bedforms, bedforms missed by TPI identification in both the manual and model output examples, and bedforms captured by model output that were missed by manual identification.